

# Double-layer nanoparticle-based coatings for efficient terrestrial radiative cooling



Hua Bao<sup>a,\*</sup>, Chen Yan<sup>a</sup>, Boxiang Wang<sup>b</sup>, Xing Fang<sup>b</sup>, C.Y. Zhao<sup>b</sup>, Xiulin Ruan<sup>c</sup>

<sup>a</sup> University of Michigan-Shanghai Jiao Tong University Joint Institute, Shanghai Jiao Tong University, Shanghai 200240, China

<sup>b</sup> Institute of Engineering Thermophysics, School of Mechanical Engineering, Shanghai Jiao Tong University, Shanghai 200240, China

<sup>c</sup> School of Mechanical Engineering and Birck Nanotechnology Center, Purdue University, West Lafayette, IN 47907, United States

## ARTICLE INFO

### Keywords:

Radiative cooling  
Particle embedded coatings  
Multiple scattering  
Selective radiative property

## ABSTRACT

One passive cooling approach is pumping energy to outer space through thermal radiation. Such a radiative cooling mechanism widely exists in nature and is important to maintain the temperature of the earth. However, natural materials generally have poor radiative cooling efficiency. To better utilize the radiative cooling for thermal management applications, the surface should be designed to have a high reflectivity in the solar spectrum and high emissivity in the "sky window" region (8–13  $\mu\text{m}$  in wavelength). In this work, we propose and demonstrate a highly scalable nanoparticle-based double-layer coating to achieve such selective radiative properties. Double-layer coatings consisting of a top reflective layer with high solar albedo and a bottom emissive layer are achieved by properly designed  $\text{TiO}_2$ ,  $\text{SiO}_2$ , and  $\text{SiC}$  nanoparticles. These coatings were fabricated on both low- and high-emissivity substrates and their spectral radiative properties were characterized. The coating composed of  $\text{TiO}_2$  and  $\text{SiO}_2$  on a reflective substrate has excellent selective emission property for radiative cooling purpose. Under dry air conditions and assuming non-radiative heat transfer coefficient  $h_c = 4 \text{ W/m}^2 \text{ K}$ ,  $\text{TiO}_2 + \text{SiO}_2$  and  $\text{TiO}_2 + \text{SiC}$  can theoretically achieve about 17 °C below ambient at night and 5 °C below ambient under direct solar radiation (AM1.5). On-site measurements have also been conducted. Under direct solar irradiation, significant temperature reduction was observed for both aluminum and black substrate after the coating was applied. At nighttime, radiative cooling effect can cool the surface to a few degrees below ambient temperature. Although the theoretical cooling under dry weather condition is not observed, the experiment results can be well explained by theoretical calculations with the consideration of high humidity and non-radiative heat transfer. This nanoparticle-based approach can be easily applied to large area, which is a significant step of achieving large scale application of the radiative cooling technology.

## 1. Introduction

Radiative heat pumping to outer space is an important mechanism to maintain the temperature of the earth. The efficiency of radiative cooling depends on the spectral emissivity of the surface of an object. If surface emissivity can be tuned to enhance the efficiency of radiative cooling, it could be an important passive cooling approach and widely applied to thermal management of buildings [1], electronics heat dissipation [2] and cooling of solar cells [3]. Radiative cooling relies on the fact that the atmosphere transmits about 87% of the outgoing radiation from the earth in the "sky window" region (8–13  $\mu\text{m}$  in wavelength) [4]. It is possible for the surface to exchange heat with the cold outer space through the "sky window". The surfaces, which emit strongly in this wavelength region and reflect strongly beyond this region, experience an imbalance of outgoing and incoming thermal

radiation and achieve lower steady-state temperature than the ambient.

It is a common practice to apply coatings on the material surface to modify its thermal radiative properties. Recent researches on radiative cooling coatings can be divided into two categories: daytime radiative cooling and nighttime radiative cooling, and the latter neglects solar radiation. To achieve nighttime cooling, the spectrally selective coatings should emit strongly in "sky window" region. Early investigations rely on bulk and thin film materials with an intrinsic emissive peak in "sky window" region to achieve radiative cooling. Granqvist and Hjortsberg [5] evaporated  $\text{SiO}$  film on Al substrate which can theoretically achieve 40 °C below ambient temperature (assuming  $T_a = 21 \text{ }^\circ\text{C}$ ) by neglecting non-radiative heat transfer. Although a single emission peak was observed, the average emittance in "sky window" regime was only 43%. Diatezua et al. [6] deposited three silicon oxynitride multi-layers onto aluminum-coated glass substrate to obtain wide absorption

\* Corresponding author.

E-mail address: [hua.bao@sjtu.edu.cn](mailto:hua.bao@sjtu.edu.cn) (H. Bao).

peak within the “sky window” region by adjusting thickness and stoichiometry of each layer. The sample with best performance can theoretically become 52 °C below ambient temperature. The drawback of this approach is the difficulty to exactly control the optimal thickness and stoichiometry in large scale production. Gentle and Smith [4] prepared polyethylene film doped with SiC and SiO<sub>2</sub> nanoparticles. When placed on an aluminum substrate, this coating has a strong emission peak in “sky window” region. The sample with best performance can theoretically achieve 25 °C below ambient temperature (assuming  $T_a = 17$  °C) with non-radiative heat transfer coefficient  $h_c = 2$  W/m<sup>2</sup> K. In addition to solid materials, radiative cooling with gas containing selective IR emission was also reported. Eriksson and Granqvist [7] investigated the mixture of several gas with absorption peaks in the wavelength region from 7 to 20 μm, but their cooling performance was not studied and potential problem related to gas condensation was not taken into consideration. While all the above works tries to utilize the intrinsic absorption peak of materials to achieve high selective emittance, various types of metamaterials have also been recently introduced. Their emission peak can be tuned by adjusting the structural parameters. For example, Hossain et al. [8] experimentally designed an anisotropic metamaterial consisted of periodically arranged metal–dielectric conical metamaterial pillars, which strictly emit from 8 to 13 μm wavelengths. The theoretical cooling power of 116.6 W/m<sup>2</sup> at room temperature and potential of cooling 58 °C below the ambient temperature were estimated without non-radiative heat transfer.

For daytime radiative cooling, high reflectance in the solar light region is also desired, since the solar radiance was orders of magnitude larger than that emitted by the surface. In early research, pigmented coatings with high albedo in solar radiance and transparency in the IR regime were studied. For example, Nilsson and Niklasson [9] fabricated nanoparticle-embedded polyethylene film as a solar reflecting cover. However, the IR emissive property solely depends on the substrate. Recently, radiative cooler based on photonic structures has attracted many research interests. Rephaeli et al. [10] designed a metal-dielectric photonic structure which behaved as a broadband mirror for solar light, and emitted selectively in the “sky window” region. The structure consisted of two thermally emitting photonic crystal layers comprised of SiC and quartz, below which lied a broadband solar reflector consisting of three sets of five double-layers made of MgF<sub>2</sub> and TiO<sub>2</sub> with varying periods on a silver substrate. The structure only absorbs 3.5% of solar radiance and can theoretically achieve 40 °C below ambient temperature and cooling power of 105 W/m<sup>2</sup> (assuming  $T_a = 27$  °C). However, the authors did not present any experimental results, presumably due to the difficulty to fabricate such a complicated structure. Raman et al. [11] introduced a photonic radiative cooler consisting of seven alternating layers of hafnium dioxide (HfO<sub>2</sub>) and silicon dioxide (SiO<sub>2</sub>) with varying thicknesses, on top of 200 nm silver (Ag), which were deposited on a 200 mm silicon wafer. The structure absorbed only 3% of solar radiance. It was experimentally demonstrated about 5 °C below ambient temperature under direct sunlight ( $P_{\text{sun}} = 860$  W/m<sup>2</sup>) and the cooling power was about  $40.1 \pm 4.1$  W/m<sup>2</sup>. Apart from the researches discussed above, some other works [12–17], such as cooling of solar cells [15], colored preserved paints [16] with decorative appeal and wind shield [17] to preserve cooling performance, were also introduced.

Although the photonic structures can achieve good selective spectral performance, it is still quite challenging to widely apply such structures in real applications. The two major issues are the scalability and cost. With the current technology, the photonic structure can only be achieved at wafer scale. Given the moderate theoretical limit of the radiative heat pumping power ( $\sim 100$  W/m<sup>2</sup>) [18], the coating must be applied to large area (such as the entire roof of a building) to be effective. In addition, to make this technology more competitive with active cooling approach, the cost should be low. Therefore, for radiative cooling purpose, instead of seeking for best spectral emission property,

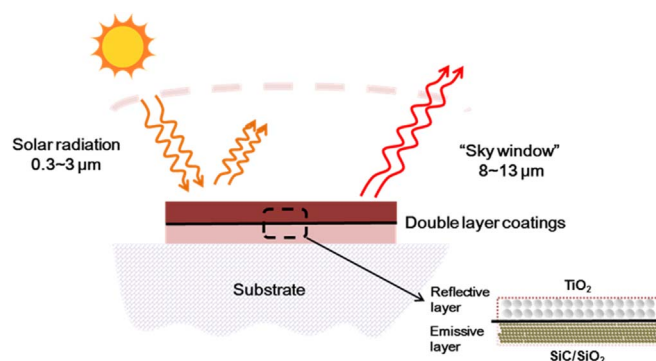


Fig. 1. Schematic of a double-layer coating design for efficient radiative cooling.

the scalability and cost are much more important. As such, new designs of thermal radiative coatings with good performance, but much less expensive and easy to prepare should be more favorable.

Motivated by such considerations, in this work, two types of double-layer coating with densely packed nanoparticles, which are more favorable for large scale application, were introduced and their radiative cooling performance was studied theoretically and experimentally. Both of them have high solar albedo, one with broad emissivity covering the whole IR region and the other with selective emissivity within “sky window” regime. We first optimized the particle size and thickness with numerical simulation methods and then the low-cost particles were deposited on different surfaces to enhance the cooling performance of substrates. Their reflectivity and emissivity were characterized, and then cooling power and stagnation temperature were studied theoretically and experimentally.

## 2. Design and fabrication

We propose a double-layer nanoparticle-based coating structure, as shown in Fig. 1. The double-layer coatings are composed of a top layer for the purpose of solar reflection and an underlying layer that has desired emissive property in the “sky window” region. The reflection layer should be highly reflective in the solar spectrum and transparent in the mid to far IR spectrum, so that the thermal emission property of double-layer coating is mainly dependent on the bottom emissive layer. To achieve such a design, the material type, the size, pile thickness, and volume fraction are carefully selected and optimized, as will be discussed below.

### 2.1. Choice of particles and preparation methods

TiO<sub>2</sub> is a common material with high refractive index, wide band gap and stable chemical properties. It is transparent to most of the infrared radiation [19]. It has been proven that submicron TiO<sub>2</sub> particles (both anatase and rutile) can scatter sun light strongly and thus work as an efficient solar reflector [20]. As such, we choose submicron rutile TiO<sub>2</sub> particles for the top reflective layer. Since the submicron size is much smaller than the wavelength of thermal radiation, these particles will not strongly scatter thermal radiation. Considering the strong scattering effect of submicron particles with high refractive index, the finite-difference time-domain (FDTD) method [21] was adopted to optimize the size and thickness of densely packed TiO<sub>2</sub> nanoparticles, which will be discussed later.

To achieve strong emission peaks in the “sky window”, one can utilize the optical phonon in ionic dielectrics that can couple strongly in this spectrum. The spectral regime of strong optical phonon coupling is also known as the Reststrahlen band of a material. For a bulk material, the Reststrahlen band is characterized by a strong reflection peak. However, if the material is made into nanoparticles, the surface phonon polariton can be induced and results in strong optical absorption (and

emission). Here we choose SiO<sub>2</sub> to achieve selective emission in the “sky window”. Although β-SiC also has Reststrahlen band in 8–13 μm, the commercial available β-SiC particles are generally broadband emitters [22]. Therefore, we choose β-SiC for the broadband emission bottom layer. In order to select proper particle sizes, we later adopted the Maxwell-Garnett-Mie (MGM) method [23], which has been widely employed to investigate the surface plasma resonance in metal nanoparticles. Afterwards the emittance was calculated with thin film model [24].

The common preparation methods of thin film are spraying coating, spinning coating and blade coating, etc. Spraying coating method [25] was adopted in our experiment because of its simple operation and potential domestic use. With the spraying coatings method, densely packed particles were deposited on the substrates.

### 2.2. Optimization of size and pile thickness

The Lumerical FDTD solutions software [26] is adopted to investigate the optical response of the disordered particles system. Due to the large computational cost of the FDTD simulation, the coating composed of densely packed particles is represented by periodic structure of simulation domain with certain size. The simulation details are shown in the Supplementary file. The modeling details and convergence tests are shown in Figs. S1–S6 (the supplementary file). The frequency dependent dielectric function of the rutile TiO<sub>2</sub> is taken from Palik [27].

To investigate the size effect of particles, we first fix the thickness to be 10 μm. As the Mie resonance peak occurs when the size parameter ( $x = 2\pi r/\lambda$ ) approximately equals 1. The scattering peak of single particle with size of 0.05–0.5 μm locates in the solar radiance region. In addition, considering the availability of particles, three typical sizes (with radius of 0.2 μm, 0.5 μm, and 1 μm) are investigated. The simulation results are as shown in Fig. 2(a). It can be observed that densely packed particles with radius of 0.5 μm have uniform high reflectance over the solar region, so the particle radius is set as 0.5 μm in further study. The reflectance for the densely packed particles with different thickness is further investigated and the results are shown in Fig. 2(b). It can be found that the reflectance is high enough when thickness is larger than 10 μm. Therefore, in the experiments, the thickness is controlled to be greater than 10 μm.

The size effect of SiO<sub>2</sub> nanoparticles with radius smaller than 1 μm (much smaller than incident wavelength) on the effective refractive index is studied with the MGM theory [28] through the relations:

$$\frac{\epsilon_{eff} - \epsilon_m}{\epsilon_{eff} + 2\epsilon_m} = \frac{f}{R^3} \alpha(r), \quad \alpha(r) = \frac{3i\lambda^3}{16\pi^3 \epsilon_m^{3/2}} a_1(r), \quad (1)$$

where  $\epsilon_m$  and  $\epsilon_{eff}$  are the dielectric constant of the matrix and the

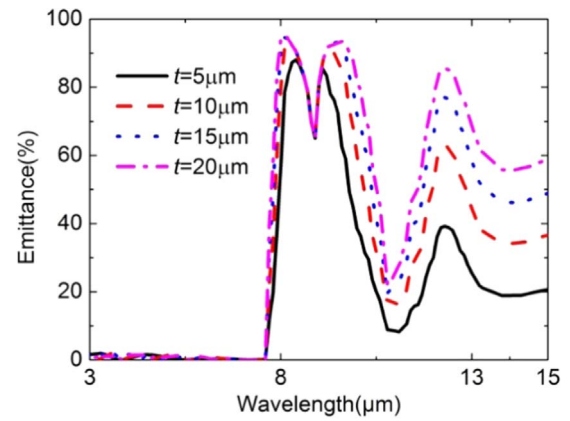


Fig. 3. Predicted emittance in the IR region of SiO<sub>2</sub> coatings with various thickness (*t*).

fictitious homogenous medium, and the dielectric constant of the particles is taken from Palik [27].  $\alpha(r)$  is the polarizability of particle which is directly related to the first electric Mie coefficient  $a_1(r)$ ,  $r$  and  $f$  are the radius and the volume fraction of the nanoparticles respectively. Based on Eq. (1), one can calculate the effective dielectric function. It can be found that for radius smaller than 300 nm, the size effect can be neglected (results not shown). With the calculated effective refractive index of the layer, the absorptance, or emittance, is obtained with the standard thin film models [24] that requires the complex refractive index and thickness of the thin film. The simulation results for different thickness are shown in Fig. 3. It can be seen that the high emittance peak in the wavelength from 8 to 11 μm does not change much while the intensity of peak near 13 μm increases with the increasing of thickness. Thus coatings with average thickness larger than 10 μm are prepared in experiment.

### 2.3. Fabrication

The coatings are prepared with spraying coating methods and the fabrication details are provided in the Supplementary file and the sketch of preparation is shown in the Fig. S7 (the supplementary file). In most of the previous investigations, a highly reflective substrate (such as Al) has been chosen to achieve selective radiative properties [4,5]. However, for real applications, the coating should be able to be applied to any type of substrate. Therefore, to demonstrate the performance of our coatings on different surface, we consider two types of substrates, one is highly reflective Al foil, and the other is an Al foil coated with a highly absorptive black paint. As shown in Fig. 4, the top three samples are Al substrate and Al substrate covered with

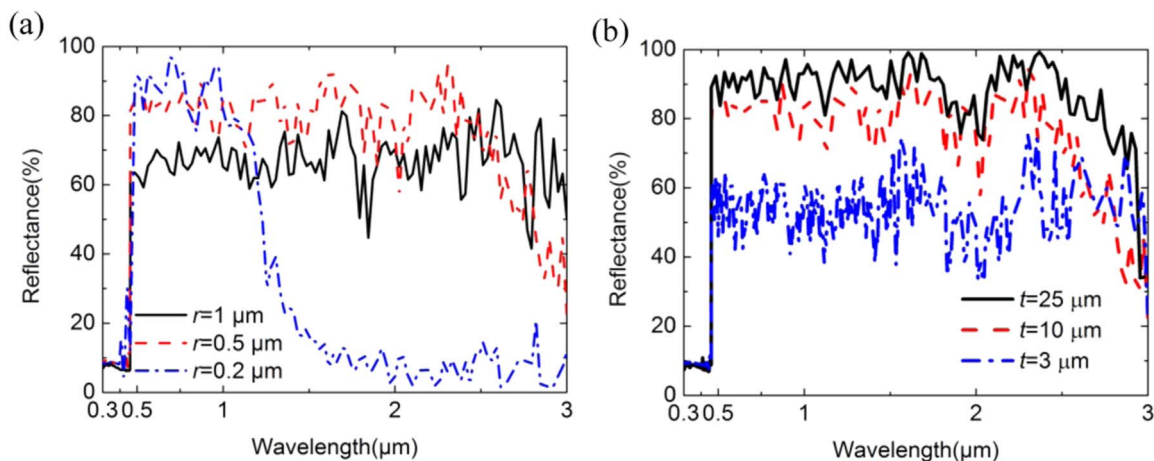


Fig. 2. Predicted reflectance spectra in the solar spectrum for random TiO<sub>2</sub> particles with (a) different sphere radius and fixed thickness  $t = 10 \mu\text{m}$  and (b) different thickness and fixed radius  $r = 0.5 \mu\text{m}$ .



Fig. 4. Substrates and substrates covered by double-layer coatings. The upper three coatings are bare Al substrate and substrate covered with different coatings. The lower ones are black substrate and substrate covered with different coatings.

different nanoparticles, while the bottom ones are black substrate and black substrate covered with different nanoparticles.

### 3. Results and discussion

#### 3.1. Spectral emittance

The spectral hemispherical reflectance ( $R$ ) from the ultraviolet to the infrared (0.3–25  $\mu\text{m}$ ) is measured by a PerkinElmer Lambda 750 spectrometer with a spectralon coated integrating sphere (0.3–3  $\mu\text{m}$ ) and a FTIR with a gold coated integrating sphere (3–25  $\mu\text{m}$ ). The spectral emittance is simply calculated by  $1-R$ , since the samples are all opaque. We first measured the spectral property of the Al and black substrate, the emissivity of Al foil is approximately zero ( $< 1\%$ ) in the whole spectral regime while that of black substrate is larger than 95%.

The spectral emittance of  $\text{TiO}_2 + \text{SiO}_2$  and  $\text{TiO}_2 + \text{SiC}$  coatings on Al substrate are shown in Fig. 5(a). The  $\text{TiO}_2 + \text{SiO}_2$  coating has quite high reflectivity from 0.5 to 8  $\mu\text{m}$  in wavelength and high emittance in the 8–18  $\mu\text{m}$  region. The  $\text{TiO}_2 + \text{SiC}$  coating has high reflectivity in the solar radiance region (0.5–3  $\mu\text{m}$ ), and high emittance in whole IR region (3–25  $\mu\text{m}$ ). The high reflectivity of both coatings in the 0.5–3  $\mu\text{m}$  region is mainly due to the strong scattering effect of  $\text{TiO}_2$  particles, which

vanishes gradually with the increase of wavelength. In the 3–11  $\mu\text{m}$  region, the upper  $\text{TiO}_2$  layer is nearly transparent to the IR radiation, and the emissivity spectra of double-layer coatings mainly depend on the underlying emissive layer. In addition, the emittance in wavelength longer than 13  $\mu\text{m}$  is also partly related to the absorption of the vibration of the Ti–O bonds [29]. For both coatings, the sharp increase of emittance below 0.46  $\mu\text{m}$  is due to the absorption of  $\text{TiO}_2$  when the incident photon energy is larger than the intrinsic bandgap ( $E_g = 3.05 \text{ eV}$  [30]). For all coatings, the emittance peak around 3  $\mu\text{m}$  is due to the water vapor adsorbed on the nanoparticles. We remark that such a spectral radiative property achieved by nanoparticles is one of the most important results of this work. Especially, the overall reflectivity of  $\text{TiO}_2 + \text{SiO}_2$  in the solar spectrum reaches 90.7% and the emittance in the “sky window” is 90.11%.

For black substrate in Fig. 5(b), the emissivity spectra of both double-layer coatings are similar, and also similar to the  $\text{TiO}_2 + \text{SiC}$  on Al foil. Since the underlying black substrate has high emittance over the entire spectra, the spectral property of double-layer coatings is mainly related to the reflection of the top  $\text{TiO}_2$  layer.

#### 3.2. Theoretical cooling performance

Consider a radiative cooler at temperature  $T$  with spectral emissivity of  $\epsilon(\lambda)$  and exposed to a clear sky. It is subject to both solar radiance and atmospheric radiation. The cooling power of the surface is the outgoing radiance per area surface, which can be calculated with [11]:

$$P_{cool}(T) = P_{rad}(T) - P_{atm}(T_{amb}) - P_{sun} - P_{nonrad}, \quad (2)$$

the radiance emitted by the surface is [11]:

$$P_{rad}(T) = \int_0^\infty \epsilon(\lambda) E_b(\lambda, T) d\lambda, \quad (3)$$

where  $E_b(\lambda, T)$  is the spectral blackbody radiance of surface at temperature of  $T$ ,  $\epsilon(\lambda)$  is the spectral emissivity of the radiative cooler. The absorbed power due to incident atmospheric thermal radiation is [11]:

$$P_{atm}(T_{amb}) = 2\pi \int_0^{\frac{\pi}{2}} \int_0^\infty \epsilon(\lambda) \epsilon_{atm}(\lambda, \theta) E_b(\lambda, T_{amb}) d\lambda \cos \theta d\theta, \quad (4)$$

where  $E_b(\lambda, T_{amb})$  is the spectral blackbody radiance of atmosphere at temperature of  $T_{amb}$ . The spectral directional emissivity of atmosphere  $\epsilon_{atm}(\lambda, \theta) = 1 - t(\lambda, 0)^{1/\cos \theta}$ , and  $t(\lambda, 0)$  is the atmospheric transmittance in the zenith direction. The incident solar power absorbed by the structure is [11]:

$$P_{sun} = \int_0^\infty \epsilon(\lambda) E_{AM10.5}(\lambda) d\lambda, \quad (5)$$

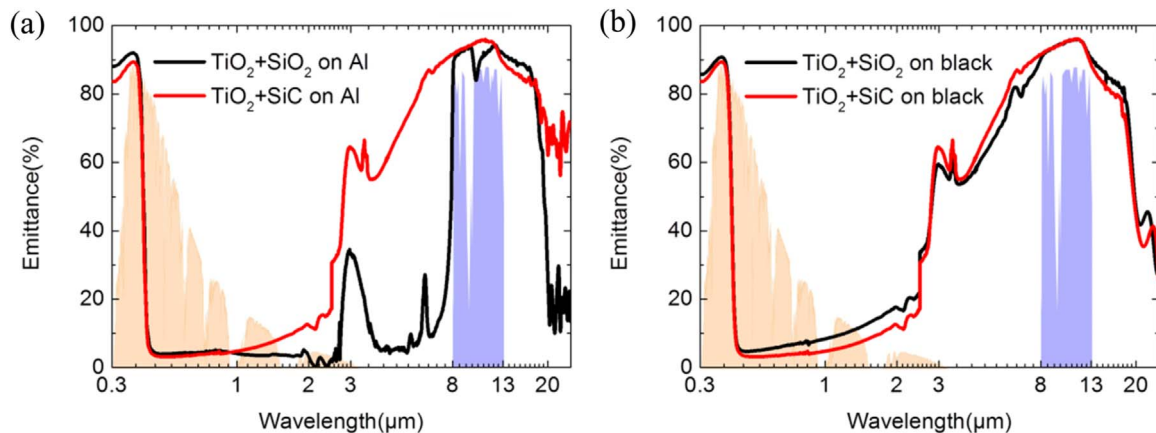


Fig. 5. Measured emissive spectra of different nanoparticles from the ultraviolet to the infrared. (a) The coatings are deposited on Al foil. (b) The coatings are deposited on black substrate.

where  $E_{AM1.5}(\lambda)$  is the solar radiance and the integration of  $E_{AM1.5}(\lambda)$  over 0.3–4  $\mu\text{m}$  region is about 1000  $\text{W}/\text{m}^2$ . The power lost due to convection and conduction is [11]:

$$P_{\text{nonrad}} = h_c(T_{\text{amb}} - T), \quad (6)$$

where  $T_{\text{amb}}$  is the temperature of the ambient and  $h_c$  is the non-radiative heat transfer coefficient containing the conduction and convection effect.

To quantify the radiative cooling performance of our spectral selective coatings, we perform theoretical calculations at different surface temperature  $T$ . The following assumptions have been made. First, since the radiative cooling is more important in tropical zone, we assume a high ambient temperature  $T_{\text{amb}} = 30^\circ\text{C}$ . Second, since the typical non-radiative heat transfer coefficient  $h_c$  is 2–6.9  $\text{W}/\text{m}^2\text{K}$  [18], we assume non-radiative heat transfer coefficient  $h_c = 4 \text{ W}/\text{m}^2\text{K}$  in the following calculation. In addition, we also calculate the cooling power of double-layer coatings without non-radiative heat transfer ( $h_c = 0$ ) for comparison. The spectral transmittance of the atmosphere is obtained from Ref. [4]. Note that the spectral transmittance is related to the humidity of the air [31], and here very dry air is assumed. The AM1.5 solar radiance is assumed [32]. The calculated relation between cooling power and temperature difference is given in Fig. 6. Since the radiative cooling performance is a function of surface temperature, two parameters are especially important to quantify the performance. One is the stagnation temperature, defined as the lowest temperature the surface can reach (corresponding to the temperature at which the cooling power is zero). The other is the cooling power when the temperature is the same as ambient.

Fig. 6(a) shows the radiative cooling performance of the coatings at nighttime for different coating temperature. For coating on Al foil,  $\text{TiO}_2 + \text{SiC}$  coating has larger cooling power (about 150  $\text{W}/\text{m}^2$ ) when the surface temperature is the same as ambient. Both coatings can reach the similar stagnation temperature, about  $17^\circ\text{C}$  below ambient. In addition, if the non-radiative heat transfer can be avoided (if  $h_c = 0$ ), the  $\text{TiO}_2 + \text{SiO}_2$  can achieve  $45^\circ\text{C}$  below ambient and  $\text{TiO}_2 + \text{SiC}$  can achieve  $35^\circ\text{C}$  below ambient. On a black substrate, since the spectral emissivity of both double-layer coatings are similar, only the calculation result of  $\text{TiO}_2 + \text{SiC}$  is presented. Since the coatings on black substrate have similar spectra as  $\text{TiO}_2 + \text{SiC}$  on Al foil, their cooling performance is also similar to that of  $\text{TiO}_2 + \text{SiC}$  on Al foil.

Fig. 6(b) shows the radiative cooling performance of the coatings at daytime for different surface temperature. On Al substrate, the  $\text{TiO}_2 + \text{SiO}_2$  and  $\text{TiO}_2 + \text{SiC}$  can achieve about  $5^\circ\text{C}$  below ambient under direct sun light (AM1.5). In addition, if the non-radiative heat transfer can be avoided (if  $h_c = 0$ ), the  $\text{TiO}_2 + \text{SiO}_2$  can achieve  $11.5^\circ\text{C}$  below ambient and  $\text{TiO}_2 + \text{SiC}$  can achieve  $10.5^\circ\text{C}$  below ambient. On black substrate, both coatings show similar coatings performance as the

$\text{TiO}_2 + \text{SiC}$  on Al, since their spectra are similar. The daytime cooling performance can be further enhanced by increasing the solar albedo of reflective layer.

In different researches, different ambient conditions are assumed to evaluate the cooling power. In order to make a direct comparison of our results with existing literature [4,11], we also theoretically calculate the performance of our coating with the conditions assumed in the literature. In Fig. 7(a), the nighttime radiative cooling performance is evaluated at  $T_{\text{amb}} = 17^\circ\text{C}$ , to be comparable with the nanoparticle coating of Gentle's [4]. Our double-layer coating has better performance in terms of output power. It should be mentioned that Gentle's coating is designed only for nighttime cooling purpose, while our coating can clearly outperform theirs at daytime. In Fig. 7(b), the theoretical cooling performance of our coating is compared with Raman's [11] experimental results. Here we assume  $T_{\text{amb}} = 20^\circ\text{C}$  and non-radiative heat transfer coefficient  $h_c$  to be 6.9  $\text{W}/\text{m}^2\text{K}$ . The solar radiance power is taken as  $P = 860 \text{ W}/\text{m}^2$ . Under such condition, our coating can theoretically achieve a stagnation temperature of about  $-3^\circ\text{C}$ , which is higher than their result. It should be mentioned that the comparison may not be "fair", because our results are theoretical and their results are from on-site measurement. However, we argue that our coating is fabricated with a scalable approach. It is much more practical for applications. The difference between our coating and Raman's is mainly due to the slightly higher absorption in the solar spectrum. While the overall absorption of our coating is nearly 10%, their structure is only 3%. If we artificially reduce the solar absorption of our coating from 9.25% to 3%, as the "Modified" curve shown in Fig. 7(b), our coating can theoretically achieve better cooling performance.

### 3.3. On-site measurements

To investigate the experimental cooling performance of double-layer coatings and compare with original substrates, on-site measurement has been conducted on the flat roof in Shanghai, in mid-September 2016. The typical ambient temperature is about  $24\text{--}32^\circ\text{C}$  and relative humidity is 50–70%. Note that the relative humidity has a fairly large effect on the spectral transmittance of the atmosphere and in turn the radiative cooling performance [33]. The details of the on-site measurements setup are shown in the Supplementary file.

The non-radiative heat transfer coefficient ( $h_c$ ) was first estimated. The apparatus was first covered by Al foil to block its radiative heat exchange and then electrical power was applied to the radiator, and stagnation temperature was obtained after 1.5 h. With two sets of electrical power and stagnation temperature obtained, the non-radiative heat transfer coefficient could be determined to be roughly 10  $\text{W}/$

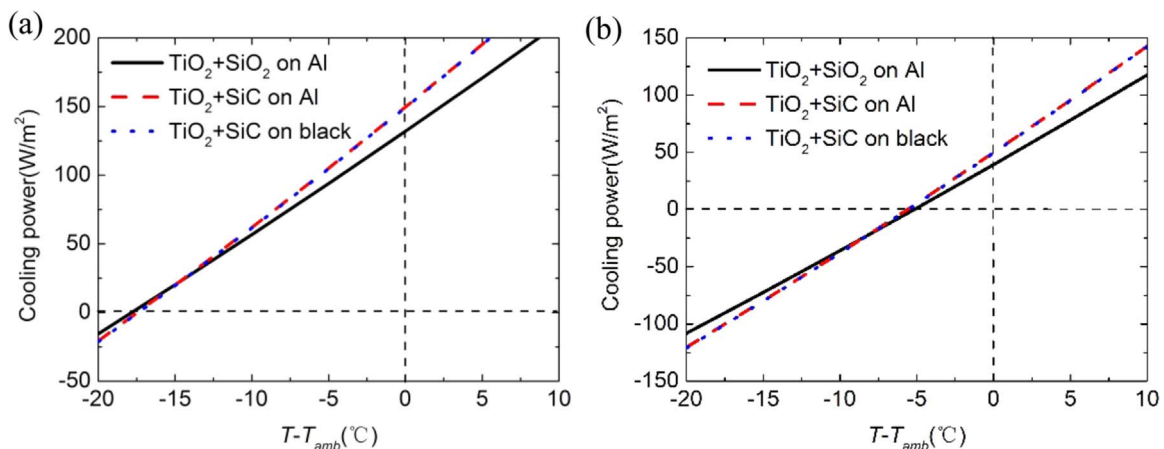


Fig. 6. Theoretical cooling power as a function of temperature difference for (a) coatings deposited on Al foil or black surface at nighttime (b) coatings deposited on Al foil or black surface under direct sunlight (AM1.5). Ambient conditions are very dry with 1.826 mm of water vapor pressure, and the non-radiative heat transfer is assumed to be 4  $\text{W}/\text{m}^2\text{K}$ .

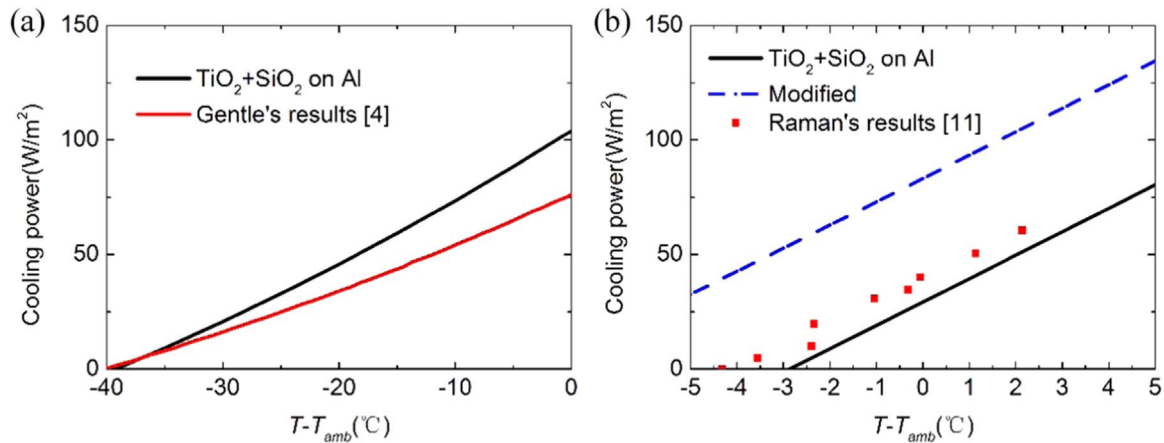


Fig. 7. The relation between cooling power and temperature difference compared between Al foil covered by  $\text{TiO}_2+\text{SiO}_2$  coatings and previous researches [4,11] at (a) nighttime with  $T_a=17^\circ\text{C}$ , (b) daytime with solar radiance of  $860\text{ W/m}^2$  and  $T_a=20^\circ\text{C}$ , assuming non-radiative heat transfer coefficient  $h_c=6.9\text{ W/m}^2\text{K}$ .

$\text{m}^2\text{K}$ . It is slightly higher than the typical values, due to the mild wind during the measurement.

To evaluate the cooling performance of double-layer coatings, Al foil and Al foil coated with black paint are chosen as two kinds of substrates. Three samples compared simultaneously are: bare substrate, substrate coated with  $\text{TiO}_2$  and  $\text{SiO}_2$ , substrate coated with  $\text{TiO}_2$  and  $\text{SiC}$ . The measurement is conducted when the electric heaters are turned off. The on-site measurement results are shown in Fig. 8.

For Al foil at daytime, the surface temperature is about  $10^\circ\text{C}$  above ambient. The application of  $\text{TiO}_2+\text{SiC}$  can cool the surface by  $8^\circ\text{C}$  and about  $2\text{--}3^\circ\text{C}$  lower than  $\text{TiO}_2+\text{SiO}_2$ . Under relatively small solar heat flux, the  $\text{TiO}_2+\text{SiC}$  coating can achieve similar temperature as ambient. It is not surprising that the  $\text{TiO}_2+\text{SiC}$  seems to perform slightly better than  $\text{TiO}_2+\text{SiO}_2$  coating, because when the surface temperature is higher than ambient,  $\text{TiO}_2+\text{SiC}$  has larger emission heat flux compared to  $\text{TiO}_2+\text{SiO}_2$ . At nighttime, the surface coated with  $\text{TiO}_2+\text{SiO}_2$  can achieve lowest stagnation temperature, about  $5^\circ\text{C}$  lower than ambient and  $1\text{--}2^\circ\text{C}$  lower than  $\text{TiO}_2+\text{SiC}$ . Since the surface temperature could be lower than ambient at nighttime, the  $\text{TiO}_2+\text{SiO}_2$  coating with a selective emissivity peak in “sky window” is able to achieve lower temperature.

On the other hand, for black surface at daytime, the surface temperature can be more than  $40^\circ\text{C}$  higher than ambient at noon. Surface coated with double-layer films had similar temperature, about  $30^\circ\text{C}$  cooler than the original black surface, but still  $3\text{--}10^\circ\text{C}$  higher than ambient, depending on the solar irradiance. At nighttime, radiators had similar cooling performance, about  $4^\circ\text{C}$  below ambient,

and the double-layer of  $\text{TiO}_2$  and  $\text{SiO}_2$  was about  $0.5\text{--}1^\circ\text{C}$  lower than another coatings. Since the spectral emissivity of two coatings on black substrate is similar over the whole spectra region ( $0.3\text{--}15\ \mu\text{m}$ ) and mainly related to the top  $\text{TiO}_2$  layer, their cooling performance is similar.

The application of double-layer coatings can significantly cool the original surface down. Unfortunately the theoretically predicted cooling to temperature below ambient is not observed under direct solar radiation. It is mainly caused by the relatively high humidity of atmosphere [31], and the always partly cloudy sky in Shanghai. To quantify the influence of humidity and cloudiness on cooling performance, with the given model from Berger's work [33] and Argiriou's research [34], the emissivity of the atmosphere is calculated with the given air temperature, relative humidity and the amount of cloud. When the relative humidity is set as 60% and cloud amount is 0.5, the emissivity of atmosphere is about 20% higher than that when we set the relative humidity as 2% and cloud amount of 0, and the emission power from the atmosphere is  $96\text{ W/m}^2$  higher, which is relatively greater value compared to the emission power of emitters. By considering the above mentioned effect and assuming the solar radiance is AM1.5 at noon and the non-radiative heat transfer  $h_c=6\text{--}12\text{ W/m}^2\text{K}$ , we recalculate the theoretical stagnation temperature of double-layer coatings.  $\text{TiO}_2+\text{SiO}_2$  can theoretically achieve  $3\text{--}5^\circ\text{C}$  above ambient at noon and  $4\text{--}6^\circ\text{C}$  below ambient at night, while  $\text{TiO}_2+\text{SiC}$  can theoretically achieve  $2\text{--}4^\circ\text{C}$  above ambient at noon and  $3\text{--}5^\circ\text{C}$  below ambient at night. The re-calculation results can well explain the experiment results under moist air condition.

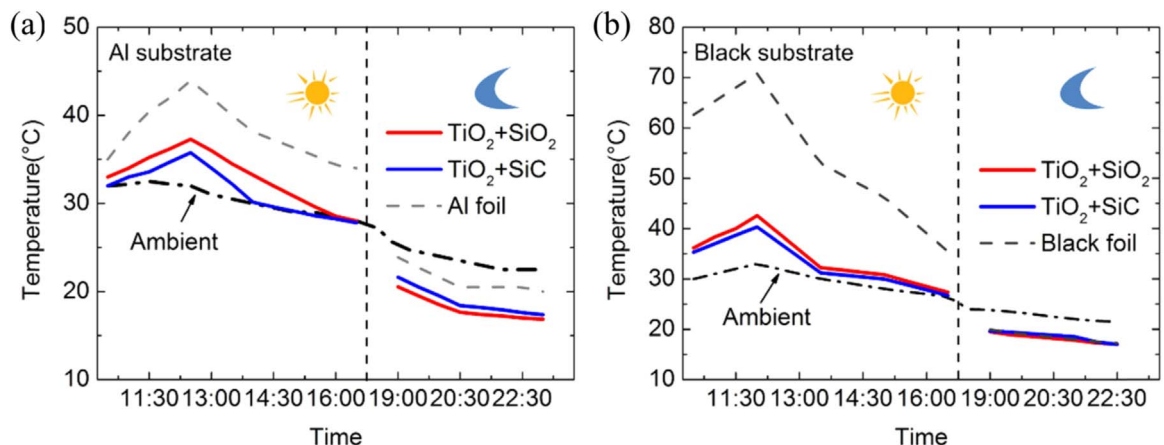


Fig. 8. Comparison between different coatings on (a) Al foil (b) black painted surface. The apparatus is placed under direct sunlight on the roof-top in Shanghai, in mid-September 2016. The typical ambient temperature is about  $24\text{--}32^\circ\text{C}$  and relative humidity is  $50\text{--}70\%$ .

#### 4. Summary and outlook

In summary, double-layer coatings composed of densely packed  $\text{TiO}_2$  particles on top of densely packed  $\text{SiO}_2$  or  $\text{SiC}$  nanoparticles, which can enhance the cooling performance of substrates, are proposed and demonstrated in this work. Simulation results show that an ideal radiator cooler should have  $\text{TiO}_2$  particles with radius of 0.5  $\mu\text{m}$  and  $\text{SiO}_2/\text{SiC}$  with radius smaller than 300 nm. On Al substrate, the overall reflectivity of  $\text{TiO}_2 + \text{SiO}_2$  in the solar spectrum reaches 90.7% and the emittance in the “sky window” is 90.11%. Under dry air condition and assuming non-radiative heat transfer coefficient  $h_c = 4 \text{ W/m}^2 \text{ K}$ , we calculate the cooling power of these coatings with the measured spectral emissivity.  $\text{TiO}_2 + \text{SiO}_2$  and  $\text{TiO}_2 + \text{SiC}$  can theoretically achieve 17 °C below ambient at night and 5 °C below ambient under direct solar radiation (AM1.5). On a black substrate, the cooling performance depends on the solar reflection ability of the  $\text{TiO}_2$  coating. Rooftop measurements in Shanghai show that both  $\text{TiO}_2 + \text{SiC}$  and  $\text{TiO}_2 + \text{SiO}_2$  can cool the Al substrate to a temperature similar or only a few degrees above ambient under direct sunlight. Both coatings can achieve about 5 °C below ambient at night. After the application, double-layer coatings can cool the Al foil for 8 °C at daytime and 5 °C at nighttime, and cool the black surface for more than 30 °C at daytime. The theoretically predicted cooling with the assumed dry air condition is not observed, which is mainly due to the high humidity of Shanghai. Despite that, our results show a new design to achieve relatively low-cost (the cost of nanoparticles is about \$7 per square meter) and scalable production of coatings for radiative cooling purpose, which has significant potential for future application at large scale.

#### Acknowledgments

The work is supported by National Natural Science Foundation of China (NO. 51636004).

#### Appendix A. Supporting information

Supplementary data associated with this article can be found in the online version at <http://dx.doi.org/10.1016/j.solmat.2017.04.020>.

#### References

- [1] L. Zhu, A. Raman, S. Fan, Color-preserving daytime radiative cooling, *Appl. Phys. Lett.* 103 (22) (2013) 223902.
- [2] C.N. Suryawanshi, C.-T. Lin, Radiative cooling: lattice quantization and surface emissivity in thin coatings, *ACS Appl. Mater. Interfaces* 1 (2009) 1334–1338.
- [3] L. Zhu, A. Raman, K.X. Wang, M.A. Anoma, S. Fan, Radiative cooling of solar cells, *Optica* 1 (1) (2014) 32–38.
- [4] A.R. Gentle, G.B. Smith, Radiative heat pumping from the earth using surface phonon resonant nanoparticles, *Nano Lett.* 10 (2) (2010) 373–379.
- [5] C.G. Granqvist, A. Hjortsberg, Radiative cooling to low temperatures: general considerations and application to selectively emitting  $\text{SiO}$  films, *J. Appl. Phys.* 52 (6) (1981) 4205–4220.
- [6] D.M. Diatezua, P.A. Thiry, A. Dereux, R. Caudano, Silicon oxynitride multilayers as spectrally selective material for passive radiative cooling applications, *Sol. Energy Mater. Sol. Cells* 40 (3) (1996) 253–259.
- [7] T.S. Eriksson, C.G. Granqvist, J. Karlsson, Transparent thermal insulation with infrared-absorbing gases, *Sol. Energy Mater.* 16 (1) (1987) 243–253.
- [8] M.M. Hossain, B. Jia, M. Gu, A metamaterial emitter for highly efficient radiative cooling, *Adv. Opt. Mater.* 3 (8) (2015) 1047–1051.
- [9] T.M. Nilsson, G.A. Niklasson, Radiative cooling during the day: simulations and experiments on pigmented polyethylene cover foils, *Sol. Energy Mater. Sol. Cells* 37 (1) (1995) 93–118.
- [10] E. Rephaeli, A. Raman, S. Fan, Ultrabroadband photonic structures to achieve high-performance daytime radiative cooling, *Nano Lett.* 13 (4) (2013) 1457–1461.
- [11] A.P. Raman, M.A. Anoma, L. Zhu, E. Rephaeli, S. Fan, Passive radiative cooling below ambient air temperature under direct sunlight, *Nature* 515 (7528) (2014) 540–544.
- [12] G.B. Smith, Amplified radiative cooling via optimised combinations of aperture geometry and spectral emittance profiles of surfaces and the atmosphere, *Sol. Energy Mater. Sol. Cells* 93 (9) (2009) 1696–1701.
- [13] A.R. Gentle, K.L. Dybdal, G.B. Smith, Polymeric mesh for durable infra-red transparent convection shields: applications in cool roofs and sky cooling, *Sol. Energy Mater. Sol. Cells* 115 (2013) 79–85.
- [14] L. Zhu, A.P. Raman, S. Fan, Radiative cooling of solar absorbers using a visibly transparent photonic crystal thermal blackbody, *Proc. Natl. Acad. Sci. USA* 112 (40) (2015) 12282–12287.
- [15] A.R. Gentle, G.B. Smith, Is enhanced radiative cooling of solar cell modules worth pursuing? *Sol. Energy Mater. Sol. Cells* 150 (2016) 39–42.
- [16] G.B. Smith, A. Gentle, P. Swift, A. Earp, N. Mronga, Coloured paints based on coated flakes of metal as the pigment, for enhanced solar reflectance and cooler interiors: description and theory, *Sol. Energy Mater. Sol. Cells* 79 (2) (2003) 163–177.
- [17] S.N. Bathgate, S.G. Bosi, A robust convection cover material for selective radiative cooling applications, *Sol. Energy Mater. Sol. Cells* 95 (10) (2011) 2778–2785.
- [18] M. Hossain, M. Gu, et al., Radiative cooling: principles, progress, and potentials, *Adv. Sci.* (2016).
- [19] Y. Mastai, Y. Diamant, S.T. Aruna, A. Zaban,  $\text{TiO}_2$  nanocrystalline pigmented polyethylene foils for radiative cooling applications: synthesis and characterization, *Langmuir* 17 (22) (2001) 7118–7123.
- [20] W.E. Vargas, Optimization of the diffuse reflectance of pigmented coatings taking into account multiple scattering, *J. Appl. Phys.* 88 (7) (2000) 4079–4084.
- [21] P.N. Dyachenko, et al., Ceramic photonic glass for broadband omnidirectional reflection, *ACS Photonics* 1 (11) (2014) 1127–1133.
- [22] H. Mutschke, A.C. Andersen, D. Clément, T. Henning, G. Peiter, Infrared properties of  $\text{SiC}$  particles, *ArXiv Prepr. Astro-Ph9903031*, 1999.
- [23] Y. Battie, A. Resano-Garcia, N. Chaoui, Y. Zhang, A.E. Naciri, Extended Maxwell-Garnett-Mie formulation applied to size dispersion of metallic nanoparticles embedded in host liquid matrix, *J. Chem. Phys.* 140 (4) (2014) 44705.
- [24] J.E. Spanier, I.P. Herman, Use of hybrid phenomenological and statistical effective-medium theories of dielectric functions to model the infrared reflectance of porous  $\text{SiC}$  films, *Phys. Rev. B* 61 (15) (2000) 10437.
- [25] X. Zhao, X.D. He, Y. Sun, L.D. Wang, Carbon nanotubes doped  $\text{SiO}_2/\text{SiO}$  2–PbO double layer high emissivity coating, *Mater. Lett.* 65 (17) (2011) 2592–2594.
- [26] F. Lumerical, Solutions, Inc., [Httpwww Lumerical Com](http://www.lumerical.com), 2016.
- [27] E.D. Palik, *Handbook of Optical Constants of Solids*, 3 Academic Press, 1998.
- [28] W.T. Doyle, Optical properties of a suspension of metal spheres, *Phys. Rev. B* 39 (14) (1989) 9852.
- [29] D.C. Cronemeyer, Electrical and optical properties of rutile single crystals, *Phys. Rev.* 87 (5) (1952) 876.
- [30] D.S. Warren, A.J. McQuillan, Influence of adsorbed water on phonon and UV-induced IR absorptions of  $\text{TiO}_2$  photocatalytic particle films, *J. Phys. Chem. B* 108 (50) (2004) 19373–19379.
- [31] T.S. Eriksson, C.G. Granqvist, Radiative cooling computed for model atmospheres, *Appl. Opt.* 21 (23) (1982) 4381–4388.
- [32] Reference Solar Spectral Irradiance: AM1.5: (<http://rredc.nrel.gov/solar/spectra/am1.5/>).
- [33] X. Berger, A simple model for computing the spectral radiance of clear skies, *Sol. Energy* 40 (4) (1988) 321–333.
- [34] A. Argiriou, M. Santamouris, C. Balaras, S. Jeter, Potential of radiative cooling in southern Europe, *Int. J. Sol. Energy* 13 (3) (1992) 189–203.